

# Total branching ratio of the $K^-$ two-nucleon absorption in $^{12}\text{C}$

R Del Grande<sup>1,2</sup>, K Piscicchia<sup>2,1</sup>, M Cargnelli<sup>3</sup>, C Curceanu<sup>1</sup>,  
L Fabbietti<sup>4,5</sup>, J Marton<sup>3</sup>, P Moskal<sup>6</sup>, A Ramos<sup>7</sup>, A Scordo<sup>1</sup>,  
D Sirghi<sup>1</sup>, M Skurzok<sup>1,6</sup>, O Vazquez Doce<sup>4,5</sup>, S Wycech<sup>8</sup>,  
J Zmeskal<sup>3</sup>, V De Leo<sup>9,10</sup>, G Mandaglio<sup>11,12</sup>, M Martini<sup>1,13</sup>,  
E Perez Del Rio<sup>9,10</sup>, A Selce<sup>14,15</sup>, M Silarski<sup>6</sup>

<sup>1</sup> INFN - Laboratori Nazionali di Frascati, 00044 Frascati, Italy

<sup>2</sup> Centro Fermi - Museo Storico della Fisica e Centro Studi e Ricerche “Enrico Fermi”, 00184 Rome, Italy

<sup>3</sup> Stefan-Meyer-Institut für Subatomare Physik, 1090 Wien, Austria

<sup>4</sup> Excellence Cluster “Origin and Structure of the Universe”, 85748 Garching, Germany

<sup>5</sup> Physik Department E12, Technische Universität München, 85748 Garching, Germany

<sup>6</sup> Institute of Physics, Jagiellonian University, 30-348 Cracow, Poland

<sup>7</sup> Departament de Física Quàntica i Astrofísica and Institut de Ciències del Cosmos, Universitat de Barcelona, 08028 Barcelona, Spain

<sup>8</sup> National Centre for Nuclear Research, 00681 Warsaw, Poland

<sup>9</sup> Dipartimento di Fisica dell’Università “Sapienza”, 00185 Roma, Italy

<sup>10</sup> INFN Sezione di Roma, 00185 Roma, Italy

<sup>11</sup> Dipartimento di Scienze Matematiche e Informatiche, Scienze Fisiche e Scienze della Terra dell’Università di Messina, 98122 Messina, Italy

<sup>12</sup> INFN Sezione di Catania, 95123 Catania, Italy

<sup>13</sup> Dipartimento di Scienze e Tecnologie applicate, Università “Guglielmo Marconi”, 00193 Roma, Italy

<sup>14</sup> Dipartimento di Matematica e Fisica dell’Università “Roma Tre”, 00146 Roma, Italy

<sup>15</sup> INFN Sezione di Roma Tre, 00146 Roma, Italy

E-mail: raffaele.delgrande@lnf.infn.it

December 2019

## Abstract.

This work is a critical re-analysis of the results obtained by the AMADEUS collaboration, concerning the measurement of the  $K^-$  multi-nucleon absorption reactions, on a  $^{12}\text{C}$  target, in the  $\Lambda p$  final state. We show that a good estimate of the  $K^-$  two-nucleon absorption total branching ratio can be extracted, given that the measured final state interactions and conversion reactions contain information on almost all the remaining hyperon-nucleon final state combinations.

The total branching ratio of the  $K^-$  two-nucleon absorption in Carbon is found to be  $(16 \pm 3(\text{stat.}) \pm 4(\text{syst.}))\%$ , which is in agreement with recent theoretical predictions.

The missing contribution from those few channels for which a  $\Lambda\text{p}$  pair can not be detected in the final state of the interaction is also estimated.

## 1. Introduction

The AMADEUS collaboration aims to provide experimental constraints to the low-energy interaction of antikaons with nucleons. The  $\bar{K}N$  interaction is the ideal testing ground to explore the fundamental symmetries of the strong interaction. In the low-energy regime the interplay among spontaneous and explicit chiral symmetry breaking emerges, as a consequence of the large strange quark mass with respect to the  $u$  and  $d$  quark masses [1]. Motivated by colour confinement, effective field theories are introduced, having mesons and baryons as fundamental degrees of freedom instead of quarks and gluons. Due to the existence of broad resonances (the isospin  $I = 0$   $\Lambda(1405)$  and the isospin  $I = 1$   $\Sigma(1385)$ ) in the  $\bar{K}N$  sub-threshold region, chiral perturbation theory can not be applied; chiral unitary approaches are then introduced or, alternatively, phenomenological  $\bar{K}N$  potential models [2, 3, 4, 5, 6, 7, 8]. The predicted  $s$ -wave  $K^-p$  and  $K^-n$  scattering amplitudes, and the positions of the corresponding poles, are strongly model dependent [9]. The  $K^-p$  interaction at threshold is constrained by the measured shift and width of kaonic hydrogen [10] (see also Ref. [11] for a complete review); the corresponding information in the  $K^-n$  channel will be extracted from the kaonic deuterium measurement [12, 13]. Experimental information above the threshold, at low kaon momenta ( $p_K < 120$  MeV/c), is strongly demanded. Below the threshold just one measurement exists, for the modulus of the  $s$ -wave  $K^-n$  scattering amplitude [14, 15].

Recent theoretical calculations also renewed the interest for the  $K^-$  multi-nucleon absorption reactions. In Ref. [16] it is shown that  $K^-$ -nuclear optical potentials based on  $K^-N$  scattering amplitudes fail to reproduce the kaonic atoms data along the periodic table of the elements, unless a  $K^-$  multi-nucleon phenomenological potential term is added. In Ref. [17] the  $K^-$  two-nucleon ( $K^-2\text{NA}$ ) interaction process was approached by means of a microscopic description of the three body problem. The Branching Ratios (BRs) were calculated for all the hyperon-nucleon final states at various baryon densities. Important experimental tests to the models can be provided by the measurement of the  $K^-$  two, three and four nucleon absorption ( $2\text{NA}$ ,  $3\text{NA}$  and  $4\text{NA}$ ) on different nuclear targets, i.e. at various nuclear densities [18, 19, 20, 21].

In Ref. [20] the BRs and low-energy cross sections for the  $K^- 2\text{NA}$ ,  $3\text{NA}$  and  $4\text{NA}$  were extracted for  $K^-$  capture on  $^{12}\text{C}$  nuclei giving rise to  $\Lambda\text{p}$  correlated production in the final state of the interaction. The detected  $\Lambda\text{p}$  pairs can be produced in Quasi-Free (QF) processes, either with a direct  $\Lambda$  production, or as a consequence of the  $\Sigma^0 \rightarrow \Lambda\gamma$  decay. Final State Interactions (FSIs), as well as  $\Sigma N \rightarrow \Lambda N'$  conversion processes, can also occur and are found to give a dominant contribution (in agreement with the result in Ref. [22]). As described in this paper a comprehensive description of

all the contributions listed above, to the measured  $\Lambda p$  distributions, allows to extract an estimate of the total BR of the  $K^-$  2NA in Carbon. The BRs of those few final states outside the acceptance of the measurements in Ref. [20] are carefully estimated and presented in Section 3.

The paper is organised as follows: in Section 2 the results obtained in Ref. [20] are summarised; the details of the FSI and conversion processes simulations are given in Section 3, where a total 2NA BR is extracted and the few missing contributions are estimated; the conclusions are given in the Section 4.

## 2. Details of the data analysis

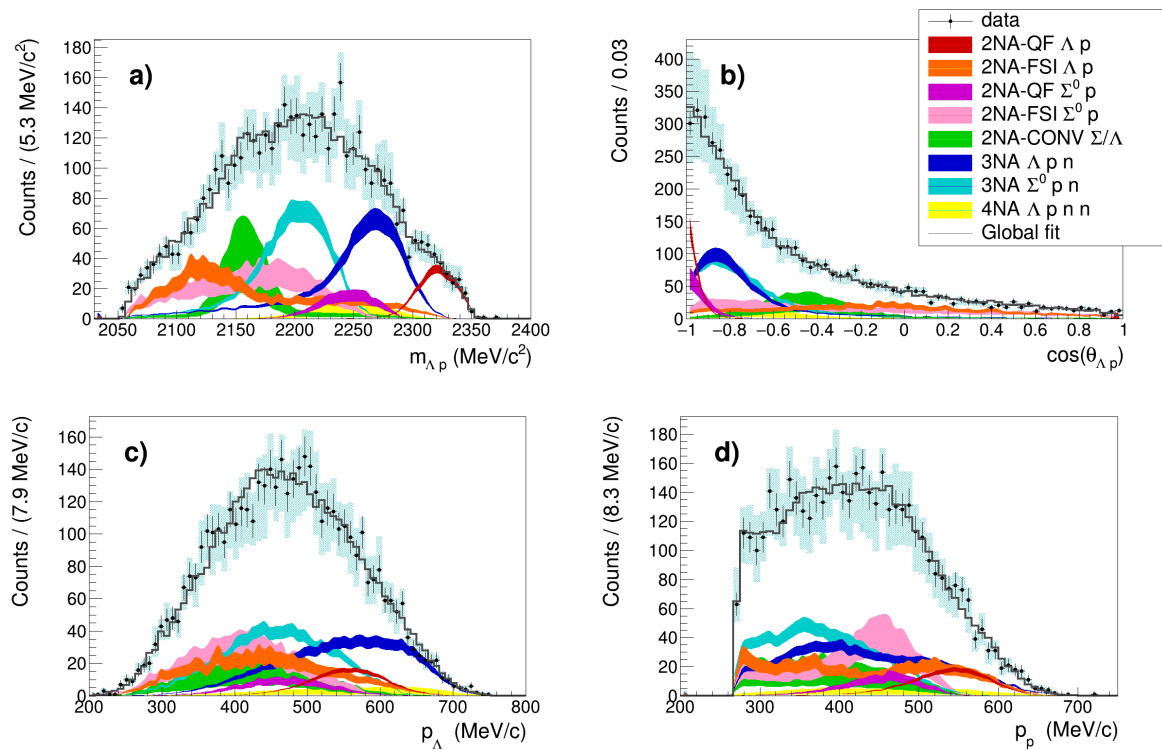
The AMADEUS collaboration is analysing the data collected with the KLOE detector during the 2004/2005 data campaign, corresponding to  $1.74 \text{ fb}^{-1}$  total integrated luminosity. Low-momentum and monochromatic  $K^-$ s ( $p_K \sim 127 \text{ MeV}/c$ ), produced at the DAΦNE collider [23] from the  $\phi$ -meson decay nearly at-rest, are absorbed in the materials of the KLOE detector [24] used as an active target. The  $K^-$  absorptions at-rest and in-flight in the nuclei contained in the beam pipe and detector materials (H,  $^4\text{He}$ ,  $^9\text{Be}$  and  $^{12}\text{C}$ ) are investigated reconstructing the emitted hyperon-pion ( $Y\pi$ ) [15] and hyperon-nucleon/nuclei ( $YN/\text{multi-N}$ ) pairs [19, 20, 21] in the final state. In Ref. [20] a pure sample of  $\Lambda p$  correlated production events was reconstructed, when the  $K^-$  is absorbed in the entrance wall of the KLOE drift chamber, which is an almost pure Carbon target. The events selection was optimised in order to reject the pionic processes, the production of a hyperon-pion pair is the signature of a  $K^-$  single-nucleon absorption. When a  $K^-$  single nucleon absorption occurs protons in the final state of the interaction can be only originated in nuclear fragmentations, such protons would be characterised by a Fermi momentum distribution. The key selection criterion is then represented by the measurement of the protons mass by Time Of Flight (TOF). For the measurement of the mass, information on the time and on the protons energy from the calorimeter is needed. The calorimeter momentum threshold ( $p_p > 240 \text{ MeV}/c$ ) efficiently discards majority of the “Fermi” protons from nuclear fragmentations. A pure sample of  $K^-$  multi-nucleon absorption processes was then selected. The detected  $\Lambda$ s can be produced (i) directly in the  $K^-$  multi-nucleon absorption (ii) as secondary products of a  $\Sigma^0$  decay ( $\Sigma^0 \rightarrow \Lambda\gamma$ ) or a  $\Sigma$  conversion ( $\Sigma N \rightarrow \Lambda N'$ ).

Monte Carlo (MC) simulations of the  $K^-$  2NA, 3NA and 4NA were performed based on Refs. [14, 25] for both the at-rest and in-flight  $K^-$  captures in  $^{12}\text{C}$  nuclei. In the case of the  $K^-$  2NA three contributions were considered: 1) the QF production of the  $\Lambda(\Sigma^0)p$  pairs, i.e. without FSIs with the residual nucleons; 2) the primary  $\Lambda(\Sigma^0)N$  production followed by elastic FSIs (only single collisions of the hyperon or the nucleon with the residual nucleus are accounted for); 3) the primary  $\Sigma N$  production followed by the inelastic  $\Sigma N \rightarrow \Lambda N'$  conversion reaction. Further details of the simulations for the processes 2) and 3) are given in Section 3.

A simultaneous  $\chi^2$  fit of the measured  $\Lambda p$  invariant mass ( $m_{\Lambda p}$ ),  $\Lambda p$  angular

correlation ( $\cos \theta_{\Lambda p}$ ),  $\Lambda$  momentum ( $p_{\Lambda}$ ) and proton momentum ( $p_p$ ) was performed. The result of the fit is shown in Fig. 1. The reduced chi-squared is  $\chi^2/dof = 194/206 = 0.94$ .

**Figure 1.**  $\Lambda p$  invariant mass (panel a),  $\Lambda p$  angular correlation (panel b),  $\Lambda$  momentum (panel c) and proton momentum (panel d) distributions are shown for the  $K^-$  absorption on  $^{12}\text{C}$  listed in the legend. Black points represent the data, black error bars correspond to the statistical errors, cyan error bars correspond to the systematic errors. The grey line distributions represent the global fitting functions, the coloured distributions represent the contributing processes according to the colour code reported in the legend and the widths correspond to the statistical error. The Figure is adapted from Ref. [20] with kind permission of The European Physical Journal (EPJ).



From the fit the BRs (for the at-rest  $K^-$  captures) and the cross sections (for the in-flight  $K^-$  captures) of all the processes contributing to the measured  $\Lambda p$  events are extracted and summarised in Table 1.

### 3. Measurement of the total 2NA branching ratio

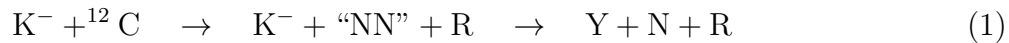
Starting from the BRs listed in Table 1 we will give an estimate of the total  $K^-$  2NA BR for captures on  $^{12}\text{C}$ ; few channels are missing in this estimate, for which we can not detect a  $\Lambda p$  pair in the final state. The missing contribution from these channels is evaluated taking advantages of the theoretical and experimental results obtained in Refs. [17, 26].

The  $K^-$  2NA-FSI and the conversion processes, used to fit the measured  $\Lambda p$

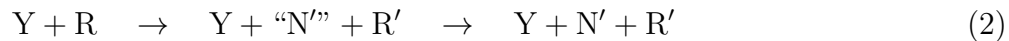
**Table 1.** Branching ratios (for the  $K^-$  absorbed at-rest) and cross sections (for the  $K^-$  absorbed in-flight) of the  $K^-$  multi-nucleon absorption processes. The  $K^-$  momentum is evaluated in the centre of mass reference frame of the absorbing nucleons, thus it differs for the 2NA and 3NA processes. The statistical and systematic errors are also given. The Table is adapted from Ref. [20] with kind permission of The EPJ.

| Process                     | Branching Ratio (%)                                | $\sigma$ (mb)                                  | @ $p_K$ (MeV/c) |
|-----------------------------|--|--|-----------------|
| 2NA-QF $\Lambda p$          | $0.25 \pm 0.02$ (stat.) $^{+0.01}_{-0.02}$ (syst.) | $2.8 \pm 0.3$ (stat.) $^{+0.1}_{-0.2}$ (syst.) | @ 128 $\pm$ 29  |
| 2NA-FSI $\Lambda p$         | $6.2 \pm 1.4$ (stat.) $^{+0.5}_{-0.6}$ (syst.)     | $69 \pm 15$ (stat.) $\pm 6$ (syst.)            | @ 128 $\pm$ 29  |
| 2NA-QF $\Sigma^0 p$         | $0.35 \pm 0.09$ (stat.) $^{+0.13}_{-0.06}$ (syst.) | $3.9 \pm 1.0$ (stat.) $^{+1.4}_{-0.7}$ (syst.) | @ 128 $\pm$ 29  |
| 2NA-FSI $\Sigma^0 p$        | $7.2 \pm 2.2$ (stat.) $^{+4.2}_{-5.4}$ (syst.)     | $80 \pm 25$ (stat.) $^{+46}_{-60}$ (syst.)     | @ 128 $\pm$ 29  |
| 2NA-CONV $\Sigma / \Lambda$ | $2.1 \pm 1.2$ (stat.) $^{+0.9}_{-0.5}$ (syst.)     | -  | -               |
| 3NA $\Lambda pn$            | $1.4 \pm 0.2$ (stat.) $^{+0.1}_{-0.2}$ (syst.)     | $15 \pm 2$ (stat.) $\pm 2$ (syst.)             | @ 117 $\pm$ 23  |
| 3NA $\Sigma^0 pn$           | $3.7 \pm 0.4$ (stat.) $^{+0.2}_{-0.4}$ (syst.)     | $41 \pm 4$ (stat.) $^{+2}_{-5}$ (syst.)        | @ 117 $\pm$ 23  |
| 4NA $\Lambda pnn$           | $0.13 \pm 0.09$ (stat.) $^{+0.08}_{-0.07}$ (syst.) | -  | -               |
| Global $\Lambda(\Sigma^0)p$ | $21 \pm 3$ (stat.) $^{+5}_{-6}$ (syst.)            | -  | -               |

distributions, were simulated as two steps reactions. The primary interaction is



where “NN” are the absorbing nucleons bound in the Carbon nucleus, R represents the residual nucleus ( $^{10}\text{Be}$  or  $^{10}\text{B}$ ), Y and N are the produced hyperon and nucleon. Two types of FSIs can give rise to the measured  $\Lambda p$  final state (the particular case of the hyperon conversion is treated separately for the sake of clarity): (i) the detected proton corresponds to the proton produced in the primary interaction (with or without having suffered re-scattering on the residual) (ii) the detected proton is a fragment of R produced in the re-scattering. The primary pairs contributing to the observed  $\Lambda p$  final state are  $\Lambda p$ ,  $\Lambda n$ ,  $\Sigma^0 p$ ,  $\Sigma^0 n$ ; the secondary interaction can then be schematically represented as:

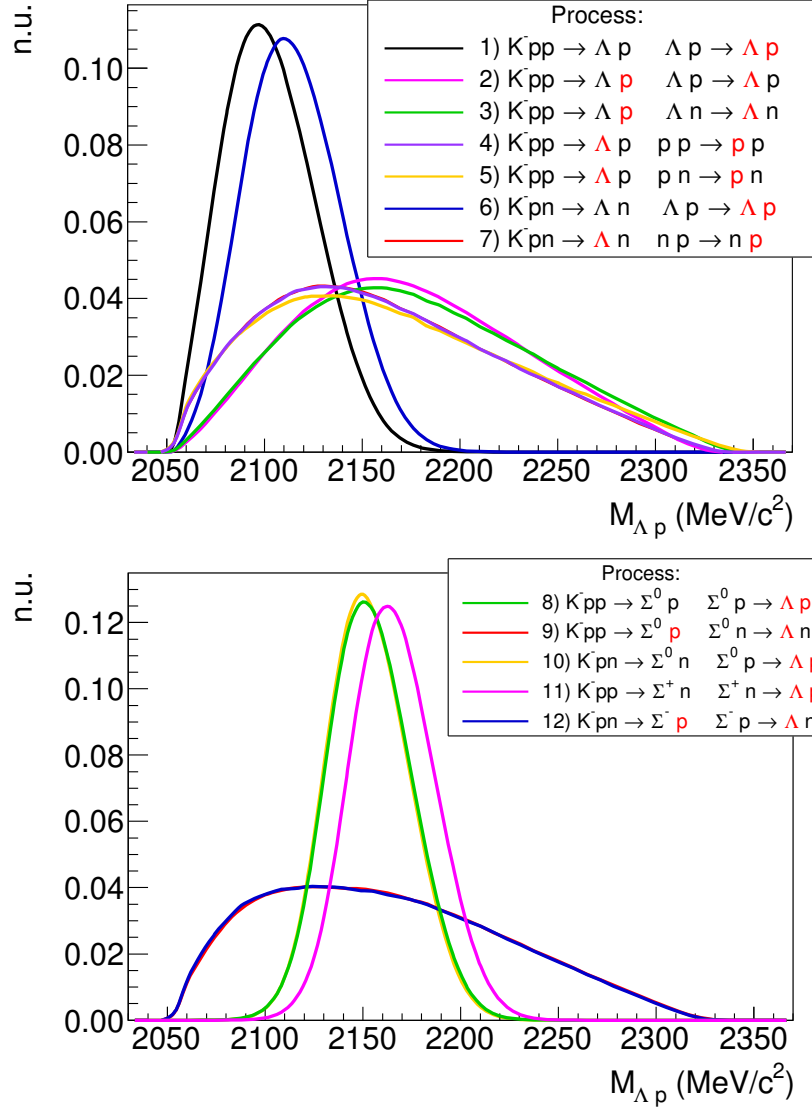


or



being  $\text{N}'$  and  $\text{R}'$  the nucleon and the residual emerging in the FSI process. The calculated  $\Lambda p$  invariant mass distributions for the  $K^-$  2NA processes producing a primary  $\Lambda N$  pair, followed by FSI and contributing to the measured  $\Lambda p$  sample are shown in Fig. 2 top panel. Left column of the legend corresponds to the primary interaction Eq. (1). Right column of the legend corresponds to the secondary interaction Eqs. (2-3). The detected particles (from which the invariant mass is built) are marked with bold red colour. The processes (1,6), (2,3) and the reactions (4,5,7) are characterised by similar shapes in all the relevant kinematic distributions; hence they are not experimentally distinguishable given the available resolutions. For these groups of similar reactions one shape is considered in the fit for each kinematic variable, corresponding to a free

**Figure 2.** Calculated invariant mass distributions for the  $\Lambda p$  pairs produced in FSI (top panel) and in the  $\Sigma/\Lambda$  conversion processes (bottom panel). The legend shows the considered elementary reactions: the primary productions according to Eq. (1) in the text (left column) and the secondary interactions as given by Eqs. (2-3) in the text (right column). The distributions refer to the  $\Lambda p$  pairs marked in bold red.



parameter. All the other processes independently contribute to the fit. The orange distribution in Fig. 1 is the weighted sum of all the independent reactions, the weights corresponding to the parameters which minimise the  $\chi^2$  function.

An analogous procedure is applied when a  $\Sigma^0$  or a charged  $\Sigma$  is produced with a nucleon in the primary interaction followed by the conversion:



The corresponding invariant mass distributions are shown in Fig. 2 bottom panel.

From the discussion above it emerges that the sum of all the BRs for the  $K^-$  2NA reactions (with or without FSIs or conversion) amounts with good approximation to the

total BR of the  $K^-$  2NA; more precisely it corresponds to the total  $K^-$  2NA BR with the following missing contributions:

- the  $\Sigma^-n$  primary production, which could give rise to the observed  $\Lambda p$  in the final state of the interaction only as a consequence of a double collision (both of the  $\Sigma^-$  and the neutron in the secondary interaction step) such a reaction was not accounted for in the analysis. The BR of this process is quoted in Ref. [17] to be about 0.1 %, which is negligible if compared with the errors in Table 1;
- the QF  $\Lambda n$  and  $\Sigma^0 n$  productions. The contributions of these reactions can be easily obtained. Given that for a nucleon momentum of the order of 560 MeV/c (typical momentum of the primarily produced nucleons) the n-n and p-n scattering cross sections are comparable, we can assume that the ratio of the QF (Ref. [20]) over the total production (Ref. [17])  $P_{\text{QF}}^{\text{YN}} = \text{BR}_{\text{QF}}(\text{YN})/\text{BR}(\text{YN})$ , is the same for the  $\Lambda n$  ( $\Sigma^0 n$ ) and  $\Lambda p$  ( $\Sigma^0 p$ ) channels. Using this ratio and the total  $\Lambda n$  and  $\Sigma^0 n$  production BRs (Ref. [17]) the BR of the QF  $\Lambda n$  and  $\Sigma^0 n$  productions is found to be globally less than 1 %;
- the FSI of primarily produced  $\Lambda n$  and  $\Sigma^0 n$  pairs without the emission of a proton in the re-scattering on the residual nucleons. The probability of the YN pairs to perform FSI with the residual nucleus can be estimated as:  $P_{\text{FSI}}^{\text{YN}} = 1 - P_{\text{QF}}^{\text{YN}} = 1 - \text{BR}_{\text{QF}}(\text{YN})/\text{BR}(\text{YN})$ . In the case of primary  $\Lambda n$  and  $\Sigma^0 n$  production the residual Boron-10 has equal amount of neutrons and protons, we then assume that the Y/N performing FSIs have 50% probability to re-scatter with a neutron. We can estimate the missing contribution as:  $\text{BR}_{\text{missing}} < \text{BR}(\Lambda n) \cdot P_{\text{FSI}}^{\Lambda n} \cdot 0.5 + \text{BR}(\Sigma^0 n) \cdot P_{\text{FSI}}^{\Sigma^0 n} \cdot 0.5 \approx 2\%$  (total BRs from Ref. [17], the inequality is motivated by the fact that the contribution of the  $\Sigma^0$  conversion should be subtracted, for which no information is available ). It is worth to notice that, whether the primary produced Y or neutron re-scatter with a neutron, a proton in the final state is always produced because a Boron-9 is left as a residual of the FSI and it is unstable with respect to the proton emission reaction:  ${}^9\text{B} \rightarrow p + {}^2\text{He}$  (the mean lifetime is of about  $10^{-20}\text{s}$  [27]). According to a dedicated simulation we estimate the maximum momentum achieved by these protons to be less than about 130 MeV/c. The experimental detection efficiency for such low momentum protons is negligible due to the mass requirement by TOF;
- the contribution due to the  $\Sigma^+$  and  $\Sigma^-$  hyperons which do not convert into a  $\Lambda$  hyperon. It is not trivial to estimate this contribution because all the conversion probabilities quoted in literature refer to the conversion of charged  $\Sigma$ s which are produced in  $K^-$  single nucleon absorptions. We then take as a reference value a conversion probability (for both  $\Sigma^+$  and  $\Sigma^-$  particles) of about 0.62 (see Ref. [26]). As a consequence the probability of non-conversion is about 0.38, multiplying this value for the corresponding BRs calculated in Ref. [17] the total contribution of these channels amounts to 3.5%;

To conclude we estimate the total BR of the  $K^-$  2NA due to  $K^-$  capture on  $^{12}\text{C}$  to be:

$$\text{BR}(K^-2\text{NA} \rightarrow \text{YN}) = (16 \pm 3(\text{stat.})_{-5}^{+4}(\text{syst.}))\% , \quad (5)$$

this is given by the sum of the BRs of all the  $K^-$  2NA reactions listed in Table 1 and misses a contribution less than 6.6 % which is comparable with the quoted error. The BR in Eq. (5) is in agreement with the total ratio for the  $K^-$  2NA process obtained in Ref. [17] which is calculated at a density of  $0.3 \rho_0$ , relevant for the low-energy capture of negatively charged kaons on  $^{12}\text{C}$ .

#### 4. Conclusions

In this work the total  $K^-$  two-nucleon absorption ( $K^-2\text{NA}$ ) Branching Ratio (BR) in  $^{12}\text{C}$  is estimated based on the measurement of the corresponding ratios having a  $\Lambda p$  in the final state given in Ref. [20]. This is made possible by the fact that final state interactions and  $\Sigma/\Lambda$  conversion processes (carefully quantified in Ref. [20]) dominate in the observed  $\Lambda p$  final state thus containing rich information on almost all the remaining hyperon-nucleon final state combinations.

The total BR of the  $K^-$  2NA in Carbon is found to be  $(16 \pm 3(\text{stat.})_{-5}^{+4}(\text{syst.}))\%$ , which is in agreement with recent prediction in Ref. [17] at  $0.3 \rho_0$  baryon density, which is the relevant density region for the absorption of low-energy  $K^-$  on  $^{12}\text{C}$  nuclei. The missing contribution from those few channels for which a  $\Lambda p$  pair can not be detected in the final state of the interaction is also estimated.

#### Acknowledgements

We acknowledge the KLOE/KLOE-2 Collaboration for their support and for having provided us the data and the tools to perform the analysis presented in this paper. Part of this work was supported by Ministero degli Affari Esteri e della Cooperazione Internazionale, Direzione Generale per la Promozione del Sistema Paese (MAECI), Strange Matter project PRG00892; EU STRONG-2020 project (grant agreement No 824093); Polish National Science Center through grant No. UMO-2016/21/D/ST2/01155.

#### References

- [1] W. Weise. Topics in low-energy QCD with strange quarks. *Hyperfine Interact.*, 233:131–140, 2015.
- [2] Y. Ikeda, T. Hyodo, and W. Weise. Chiral SU(3) theory of antikaon-nucleon interactions with improved threshold constraints. *Nucl. Phys.*, A881:98–114, 2012.
- [3] A. Cieply and J. Smejkal. Chirally motivated  $\bar{K}N$  amplitudes for in-medium applications. *Nucl. Phys.*, A881:115–126, 2012.
- [4] Zhi-Hui Guo and J. A. Oller. Meson-baryon reactions with strangeness -1 within a chiral framework. *Phys. Rev.*, C87(3):035202, 2013.
- [5] M. Mai and Ulf-G. Meißner. Constraints on the chiral unitary  $\bar{K}N$  amplitude from  $\pi\Sigma K^+$  photoproduction data. *Eur. Phys. J.*, A51(3):30, 2015.



- [6] A. Feijoo, V. Magas, and A. Ramos.  $S=1$  meson-baryon interaction and the role of isospin filtering processes. *Phys. Rev.*, C99(3):035211, 2019.
- [7] Y. Akaishi and T. Yamazaki. Nuclear anti-K bound states in light nuclei. *Phys. Rev.*, C65:044005, 2002.
- [8] L R Staronski and S Wycech. Nuclear absorption of  $K^-$  and models of  $\Lambda(1405)$ . *Journal of Physics G: Nuclear Physics*, 13(11):1361–1373, nov 1987.
- [9] A. Cieplý, M. Mai, Ulf-G. Meißner, and J. Smejkal. On the pole content of coupled channels chiral approaches used for the  $\bar{K}N$  system. *Nucl. Phys.*, A954:17–40, 2016.
- [10] M. Bazzi et al. A new measurement of kaonic hydrogen X-rays. *Phys. Lett.*, B704:113, 2011.
- [11] C. Curceanu et al. The modern era of light kaonic atom experiments. *Rev. Mod. Phys.*, 91:025006, Jun 2019.
- [12] C. Curceanu et al. Kaonic Deuterium Measurement with SIDDHARTA-2 on DAΦNE. *Acta Phys. Polon.*, B51:251, 2020.
- [13] M. Bazzi et al. Preliminary study of kaonic deuterium x-rays by the siddharta experiment at dane. *Nuclear Physics A*, 907:69 – 77, 2013.
- [14] K. Piscicchia, S. Wycech, and C. Curceanu. On the  $K^-^4\text{He} \rightarrow \Lambda\pi^-^3\text{He}$  resonant and non-resonant processes. *Nucl. Phys.*, A954:75–93, 2016.
- [15] K. Piscicchia et al. First measurement of the  $K^-n \rightarrow \Lambda\pi^-$  non-resonant transition amplitude below threshold. *Phys. Lett.*, B782:339–345, 2018.
- [16] E. Friedman and A. Gal.  $K^-N$  amplitudes below threshold constrained by multinucleon absorption. *Nucl. Phys.*, A959:66–82, 2017.
- [17] J. Hrtánková and A. Ramos. Single- and two-nucleon antikaon absorption in nuclear matter with chiral meson-baryon interactions. arXiv:1910.01336 [nucl-th], to appear in *Phys. Rev. C*, 2019.
- [18] M. Agnello et al.  $\Sigma^-p$  emission rates in  $K^-$  absorptions at rest on  $^6\text{Li}$ ,  $^7\text{Li}$ ,  $^9\text{Be}$ ,  $^{13}\text{C}$  and  $^{16}\text{O}$ . *Phys. Rev.*, C92(4):045204, 2015.
- [19] O. Vázquez Doce et al.  $K^-$  absorption on two nucleons and  $ppK^-$  bound state search in the  $^0p$  final state. *Phys. Lett.*, B758:134–139, 2016.
- [20] R. Del Grande et al.  $K^-$  multi-nucleon absorption cross sections and branching ratios in  $\Lambda p$  and  $\Sigma^0 p$  final states. *Eur. Phys. J.*, C79(3):190, 2019.
- [21] K. Piscicchia et al. Investigation of the low-energy kaons hadronic interactions in light nuclei by amadeus. *EPJ Web Conf.*, 137:09005, 2017.
- [22] V. K. Magas, E. Oset, A. Ramos, and H. Toki. A Critical view on the deeply bound  $K^-pp$  system. *Phys. Rev.*, C74:025206, 2006.
- [23] A. Gallo et al. DAFNE status report. *Conf. Proc.*, C060626:604–606, 2006.
- [24] F. Bossi et al. Precision Kaon and Hadron Physics with KLOE. *Riv. Nuovo Cim.*, 31:531–623, 2008.
- [25] R. Del Grande, K. Piscicchia, and S. Wycech. Formation of  $\Sigma\pi$  Pairs in Nuclear Captures of  $K^-$  Mesons. *Acta Phys. Polon.*, B48:1881, 2017.
- [26] C. Vander Velde-Wilquet et al. Determination of the branching fractions for  $K^-$ -meson absorptions at rest in carbon nuclei. *Il Nuovo Cimento A (1965-1970)*, 39(4):538–547, 1977.
- [27] G. Audi et al. The nubase2016 evaluation of nuclear properties. *Chinese Physics C*, 41(3):030001, 2017.